MaPBI3 and 2D hybrid organic-inorganic perovskite based microcavities employing periodic, aperiodic, and disordered photonic structures with light-induced tuning possibility

Optical Materials: X 12 (2021) 100105

Contents lists available at ScienceDirect

Optical Materials: X

journal homepage: www.journals.elsevier.com/optical-materials-x

$MaPBI_3$ and 2D hybrid organic-inorganic perovskite based microcavities employing periodic, aperiodic, and disordered photonic structures with light-induced tuning possibility

Michele Bellingeri [a,b,d], Francesco Scotognella [a,c,*]

[a] Dipartimento di Fisica, Politecnico di Milano, Piazza Leonardo da Vinci 32, 20133, Milano, Italy
[b] Dipartimento di Scienze Matematiche, Fisiche e Informatiche, Università di Parma, Via G.P. Usberti, 7/a, 43124, Parma, Italy
[c] Center for Nano Science and Technology@PoliMi, Istituto Italiano di Tecnologia, Via Giovanni Pascoli, 70/3, 20133, Milan, Italy
[d] INFN, Gruppo Collegato di Parma, I-43124, Parma, Italy

ARTICLE INFO

Keywords:
Photonic microcavities
Metal halide perovskites
Photochromic polymer
Light-induced tunable structures

ABSTRACT

Inorganic-organic perovskites semiconductors are becoming increasingly interesting due to their remarkable optical properties, such as a high photoluminescence quantum yield and the possibility to show optical gain in a broad range of wavelengths. We have here simulated microcavities that embed $MaPBI_3$ and 2D hybrid organic-inorganic perovskite semiconductors by sandwiching such active layers between periodic, aperiodic and disordered photonic structures. The complex refractive index dispersions of $MaPBI_3$ and 2D hybrid organic-inorganic perovskite have been recently reported in literature. Thus, we have carefully considered the refractive index dispersion of all the materials employed, such as silicon dioxide, titanium dioxide, and the aforementioned perovskite layers. Moreover, by employing a photochromatic polymer, namely the diarylethene-based polyester pDTE, we have designed a microcavity with light-induced tuning of the cavity modes is possible.

1. Introduction

Organic-inorganic halide perovskite semiconductors have become in few years highly important in photonics due to their impressive nonlinear optical properties [1–4]. These materials are interesting because of their unique performances as photovoltaic materials, but also because of their high photoluminescence quantum yield and optical gain, making them promising for light-emitting diodes and lasers [5]. Just to cite a few examples, perovskite-based lasers have been monolithically integrated into a silicon nitride photonic circuit [6] and perovskite-based random lasing with cavity exciton-polaritons has been reported [7].

In photonics, the simplest building block is the photonic crystal [8–10], characterized by the alternation of different refractive indexes in one, two, or three directions. The one-dimensional photonic crystals are particularly interesting because they can be fabricated with a large variety of techniques [11], the optical properties can be studied with high accuracy [12], both for enhancement of spontaneous emission [13, 14] and lasers [15–19]. One-dimensional photonic structures can be designed by following aperiodic and disordered (random) patterns. These structures can be exploited to tune and enhance the optical characteristics of emitting materials embedded in such structures [20–23].

One-dimensional photonic crystals that include perovskites have been used to fabricate efficient solar cells with tunable structural colour [24]. Moreover, microcavities based on polymeric materials that embed perovskites have been designed and fabricated [25].

For a proper design of the photonic structures including perovskite semiconductors as a constituent material, it is necessary to know the real part and the imaginary part of the refractive index as a function of the wavelength, i.e. the complex refractive index dispersion. The refractive index of $MAPbI_3$ has been reported by several groups in Refs. [26–29]. Recently, also the refractive indexes of 2D hybrid organic-inorganic perovskite (HOIP) semiconductors in Ruddlesden–Popper (RP) and Dion–Jacobson (DJ) phases have been reported [30].

In this work, we have exploited the determination of the complex refractive index dispersion of these perovskite materials. With such dispersions we have simulated photonic microcavities, that embed MaPBI3 and 2D hybrid organic-inorganic perovskite semiconductors, by sandwiching such active layers between periodic, aperiodic, and

* Corresponding author. Dipartimento di Fisica, Politecnico di Milano, Piazza Leonardo da Vinci 32, 20133, Milano, Italy.
E-mail address: francesco.scotognella@polimi.it (F. Scotognella).

https://doi.org/10.1016/j.omx.2021.100105
Received 31 August 2021; Received in revised form 4 October 2021; Accepted 8 October 2021
Available online 20 October 2021

disordered photonic structures. We demonstrate the possibility to observe cavity modes with the different structures. Moreover, we demonstrate the possibility to obtain a tunable microcavity by adding layers of diarylethene-based polyester (pDTE) in the microcavity.

2. Methods

We have used the transfer matrix method [31–33] to simulate the light transmission spectra of the differently designed microcavities.

In this study, we consider a system glass/multilayer/air that is impinged by the light with normal incidence.

The multilayer system can be described as a product of matrix $\prod_{j=1}^{x} M_j = M = \begin{bmatrix} m_{11} & m_{12} \\ m_{21} & m_{22} \end{bmatrix}$ with x number of layers. The characteristic matrix of each layer M_j, with j=(1,2, …,x), is:

$$M_j = \begin{bmatrix} cos(\varphi_j) & -\frac{i}{p_j} sin(\varphi_j) \\ -ip_j sin(\varphi_j) & cos(\varphi_j) \end{bmatrix} \quad (1)$$

where the argument φ_j of the trigonometric functions in the matrix is the phase variation of the light wave passing through the jth layer, and for normal incidence $\varphi_j = (2\pi/\lambda) n_j d_j$, where n_j is the refractive index of the layer and d_j its thickness. The parameter is employed for transverse electric (TE) wave and, in particular, $p_j = \sqrt{\varepsilon_j/\mu_j}$. The parameter q_j, equal to $1/p_j$, replace p_j in the case of transverse magnetic (TM) wave (taking into account that, at normal incidence, the transmission spectra for TE and TM waves are the same).

From the final matrix M we can determine the transmission coefficient

$$t = \frac{2p_s}{(m_{11} + m_{12}p_0)p_s + (m_{21} + m_{22}p_0)} \quad (2)$$

in which p_s is for the substrate and p_0 is for air. Consequently, the transmission:

$$T = \frac{p_0}{p_s}|t|^2 \quad (3)$$

The dispersion of the refractive index for SiO_2 has been taken from Ref. [34]:

$$n^2_{SiO_2}(\lambda) - 1 = \frac{1.9558\lambda^2}{\lambda^2 - 0.15494^2} + \frac{1.345\lambda^2}{\lambda^2 - 0.0634^2} + \frac{10.41\lambda^2}{\lambda^2 - 27.12^2} \quad (4)$$

While the dispersion of the refractive index of TiO_2 has been taken from Ref. [35]:

$$n_{TiO_2}(\lambda) = \left(4.99 + \frac{1}{96.6\lambda^{1.1}} + \frac{1}{4.60\lambda^{1.95}}\right)^{1/2} \quad (5)$$

The complex refractive index dispersion has been taken from Refs. [28,29], while the refractive index dispersions for two-dimensional hybrid organic-inorganic perovskite semiconductors (Ruddlesden-Popper (RP) phase and Dion-Jacobson (DJ) phase) have been taken from Ref. [30].

3. Results and discussion

We have designed three different microcavities, characterized by perovskite layers embedded between two periodic photonic crystals, two aperiodic photonic crystals, or two disordered photonic structures. We have employed three different types of perovskite semiconductors: $MAPbI_3$, monolayered Ruddlesden-Popper (RP) phase, and monolayered Dion-Jacobson (DJ) phase. In particular, the first two are largely under current investigation in the research community and hence an interesting platform for study. Instead, the DJ is an alternative two-dimensional phase that is processed similar to the RP perovskites. We chose the three types of photonic crystals to highlight the peculiarities of these sequences, which are a very precise bandgap in the case of the periodic one and a deterministic series of valleys and peaks in transmission for the aperiodic case, and random occurrence of transmission peaks in the case of disordered photonic structures.

The periodic microcavity that embeds the perovskite layer consists of a photonic crystal of 10 bilayers of $TiO_2$and SiO_2, the layer of $MAPbI_3$, another photonic crystal of 10 bilayers of TiO_2 and SiO_2 (Fig. 1a). The aperiodic microcavity consists of two Thue-Morse quasicrystals that embed the perovskite layer. Each Thue-Morse crystal is composed of 32 layers with the following sequence: ABBABAABBAABABBABAA-BABBAABBABAAB, in which A is TiO_2 and B is SiO_2 [36] (Fig. 1b). The disordered microcavity consists of two disordered photonic structures that embed the perovskite layer. Each disordered structure is composed of 32 layers in which each layer has a 50% probability of being either TiO_2 or SiO_2. The sequence of layers for the first disordered structure is BBABBAABBBABBABAABBBBABBBBBABABA, while the sequence for the second structure is AAABBABAAABBAAABBBABBAAABABABABB (Fig. 1c).

For the $MAPbI_3$-based microcavities, the thicknesses of the layers are 135 nm, 175 nm, and 350 nm, for TiO_2, SiO_2, and $MAPbI_3$, respectively. In Fig. 2 we show the transmission spectra of microcavities embedding $MAPbI_3$, with the periodic microcavity in Fig. 2 top, the aperiodic Thue-Morse microcavity in the center, and the disordered microcavity in Fig. 2 bottom.

We have simulated microcavities in which the embedded layer is the Ruddlesden-Popper (RP) phase of a two-dimensional hybrid organic-inorganic perovskite semiconductor. We have selected the monolayer of the perovskite semiconductor, that we call RP1 as in Ref. [30]. In the case of the monolayer, the formula of the compound is $(CH_3(CH_2)_3NH_3)_2PbI_2$ [30]. In Fig. 3 we show the transmission spectra of a periodic (top), an aperiodic Thue-Morse (center), and a disordered cavity (bottom). For these cavities the thickness of the titanium dioxide layers is 93 nm, the thickness of the silicon dioxide layers is 120 nm, and the thickness of the RP perovskite layer is 350 nm.

Finally, we have simulated microcavities in which the embedded layer is the Dion-Jacobson (DJ) phase of a two-dimensional hybrid organic-inorganic perovskite semiconductor. We have selected the monolayer of the perovskite semiconductor, that we call DJ1 as in Ref. [30]. In the case of the monolayer, the formula of the compound is 4-(aminomethyl)piperidinium PbI_4 [30]. In Fig. 4 we report the transmission spectra of the DJ1 phase embedded in a periodic (top), an aperiodic (center), and a disordered cavity (bottom). The thickness of the layers for these structures with DJ1 is 120 nm, 150 nm, and 350 nm for TiO_2, SiO_2 and DJ1, respectively.

From the results of Figs. 2–4 it becomes clear that the transmission spectra of the 2D perovskites RP and DJ are dominated strongly by the transmission peaks of the photonic structures. The $MAPbI_3$ absorb up to a wavelength of 750 nm, hence only in the near-infrared part of the spectra the features due to the photonic structures are predominant.

To design a tunable structure we have employed a photochromic polymer, pDTE [37], as an additional layer to induce, upon light irradiation, a shift of the spectral feature of the microcavity. It has been reported that ultraviolet irradiation induces a change from a colourless form of pDTE to a blue form of pDTE [37]. In this case, the microcavity is composed by a 10-bilayer TiO_2–SiO_2 photonic crystal, a layer of pDTE, a layer with the monolayered RP phase, a layer of pDTE, and another 10-bilayer TiO_2–SiO_2 photonic crystal. In Fig. 5 we show the transmission spectra of the cavity in the case of the transparent phase of pDTE (black solid curve) and in the case of the blue phase of pDTE (red dashed curve).

The complex refractive index of pDTE in the two forms has been taken from Ref. [37]. The transmission valley centred at 600 nm for the blue form is due to the strong absorption of the form in this spectral region. We can observe a shift of 15 nm in the cavity mode at longer wavelengths (about 800 nm) due to the photochromic behaviour of

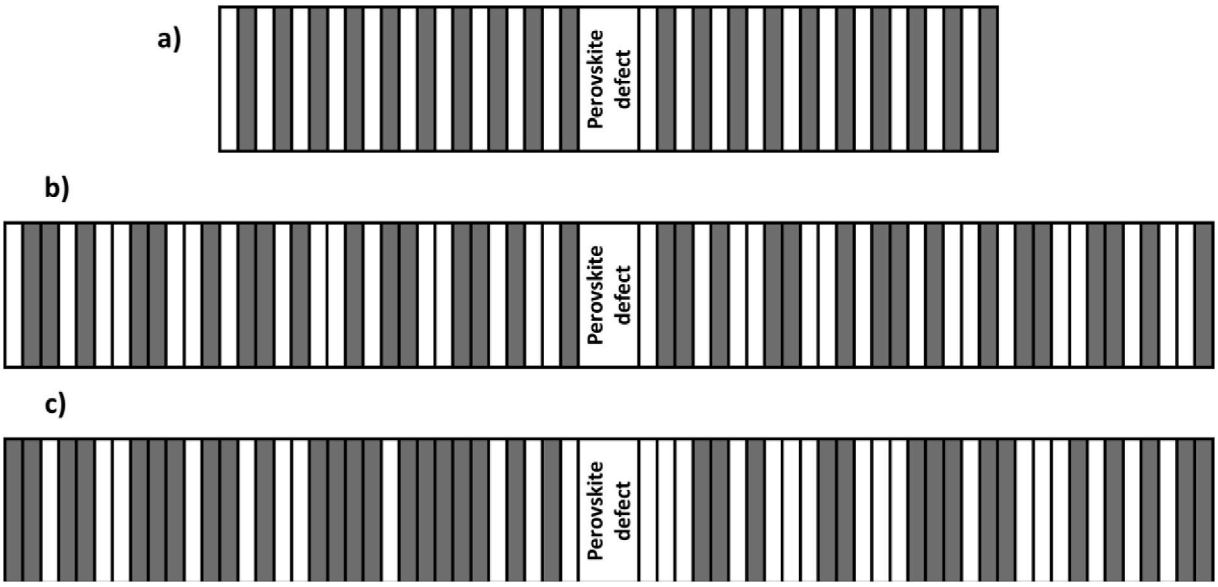

Fig. 1. Sketches of the microcavities with the perovskite layer as defect. a) Periodic microcavity; b) aperiodic microcavity; c) disordered microcavity. The white layer is TiO_2 and the black layer is SiO_2.

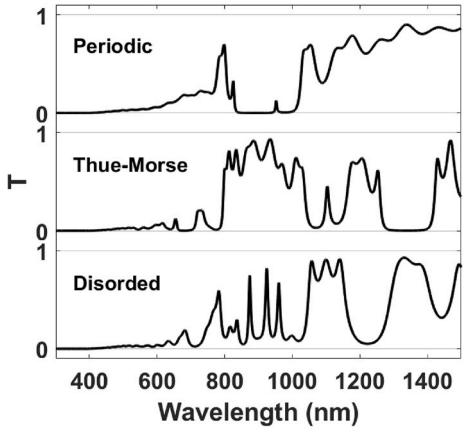

Fig. 2. Transmission spectra of the $MAPbI_3$ layer embedded in periodic, aperiodic (Thue-Morse), disordered microcavities.

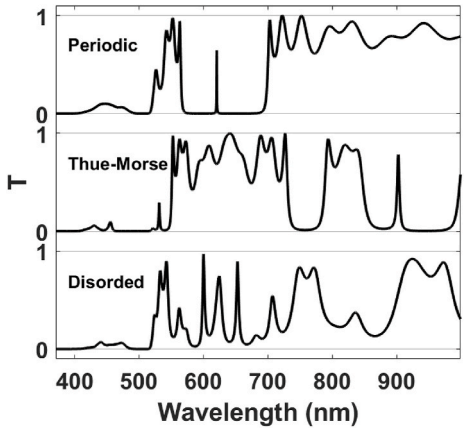

Fig. 3. Transmission spectra of the RP1 layer embedded in periodic, aperiodic (Thue-Morse), disordered microcavities.

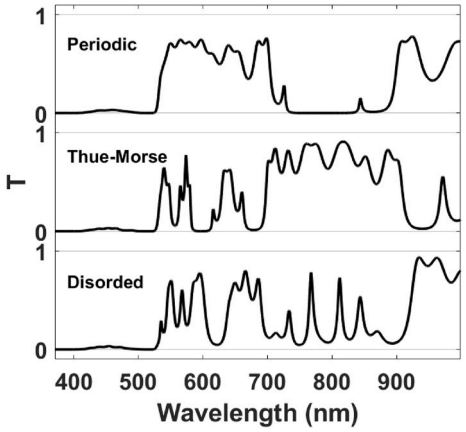

Fig. 4. Transmission spectra of the DJ1 layer embedded in periodic, aperiodic (Thue-Morse), disordered microcavities.

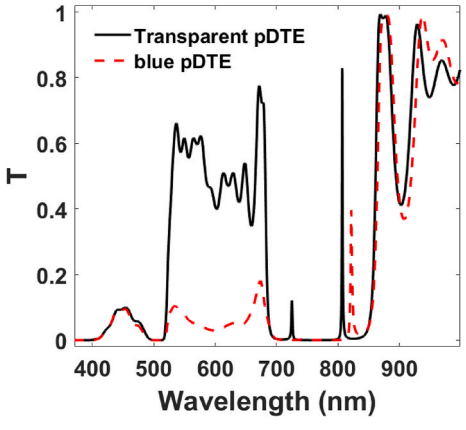

Fig. 5. Transmission spectra of the periodic cavity [(SiO_2/TiO_2)x10]/pDTE/PR1/pDTE/[(SiO_2/TiO_2)x10] with transparent phase of pDTE (black solid curve) and blue phase of pDTE (red dashed curve).

pDTE.

4. Conclusion

To conclude, we have designed a one-dimensional microcavity that embeds $MAPbI_3$ and 2D hybrid organic-inorganic perovskite semiconductors by using the transfer matrix method. Such active materials have been sandwiched between periodic, aperiodic and disordered photonic structures. To engineer the perovskite layer we have taken into account the complex refractive index dispersion of the materials, recently reported in literature, together with the refractive index dispersions of silicon dioxide and titanium dioxide. In order to conceive a tunable perovskite-based microcavity, we have employed pDTE, which is photochromic materials able to change the refractive index upon ultraviolet irradiation.

CRediT authorship contribution statement

Michele Bellingeri: Conceptualization, Methodology, Validation, Data curation, Writing – review & editing. **Francesco Scotognella:** Methodology, Validation, Data curation, Writing – original draft, Writing – review & editing, Funding acquisition.

Declaration of competing interest

The authors declare that they have no known competing financial interests or personal relationships that could have appeared to influence the work reported in this paper.

Acknowledgements

The authors thank Fondazione Cariplo for financial support (grant n° 2018-0979). This project has received funding from the European Research Council (ERC) under the European Union's Horizon 2020 research and innovation programme (grant agreement No. [816313]). Moreover, this project has received funding from the European Union's Horizon 2020 research and innovation programme under the Marie Skłodowska-Curie grant agreement no. (734690).

References

[1] G. Xing, N. Mathews, S.S. Lim, N. Yantara, X. Liu, D. Sabba, M. Grätzel, S. Mhaisalkar, T.C. Sum, Low-temperature solution-processed wavelength-tunable perovskites for lasing, Nat. Mater. 13 (2014) 476–480, https://doi.org/10.1038/nmat3911.

[2] B.R. Sutherland, E.H. Sargent, Perovskite photonic sources, Nat. Photonics 10 (2016) 295–302, https://doi.org/10.1038/nphoton.2016.62.

[3] A.L. Alvarado-Leaños, D. Cortecchia, G. Folpini, A.R.S. Kandada, A. Petrozza, Optical gain of lead halide perovskites measured via the variable stripe length method: what we can learn and how to avoid pitfalls, Adv. Optic. Mater.. n/a (n.d.) 2001773. https://doi.org/10.1002/adom.202001773.

[4] INVITED F. Marangi, M. Lombardo, A. Villa, F. Scotognella, New strategies for solar cells beyond the visible spectral range, Opt. Mater. X 11 (2021) 100083, https://doi.org/10.1016/j.omx.2021.100083.

[5] T.K. Ng, J.A. Holguin-Lerma, C.H. Kang, I. Ashry, H. Zhang, G. Bucci, B.S. Ooi, Group-III-nitride and halide-perovskite semiconductor gain media for amplified spontaneous emission and lasing applications, J. Phys. D Appl. Phys. 54 (2021) 143001, https://doi.org/10.1088/1361-6463/abd65a.

[6] P.J. Cegielski, A.L. Giesecke, S. Neutzner, C. Porschatis, M. Gandini, D. Schall, C.A. R. Perini, J. Bolten, S. Suckow, S. Kataria, B. Chmielak, T. Wahlbrink, A. Petrozza, M.C. Lemme, Monolithically integrated perovskite semiconductor lasers on silicon photonic chips by scalable top-down fabrication, Nano Lett. 18 (2018) 6915–6923, https://doi.org/10.1021/acs.nanolett.8b02811.

[7] P. Bouteyre, H.S. Nguyen, H.S. Nguyen, J.-S. Lauret, J.-S. Lauret, G. Trippé-Allard, G. Delport, F. Lédée, H. Diab, A. Belarouci, C. Seassal, D. Garrot, F. Bretenaker, E. Deleporte, Directing random lasing emission using cavity exciton-polaritons, Opt. Express, OE. 28 (2020) 39739–39749, https://doi.org/10.1364/OE.410249.

[8] S. John, Strong localization of photons in certain disordered dielectric superlattices, Phys. Rev. Lett. 58 (1987) 2486–2489, https://doi.org/10.1103/PhysRevLett.58.2486.

[9] E. Yablonovitch, Inhibited spontaneous emission in solid-state physics and electronics, Phys. Rev. Lett. 58 (1987) 2059–2062, https://doi.org/10.1103/PhysRevLett.58.2059.

[10] J.D. Joannopoulos (Ed.), Photonic Crystals: Molding the Flow of Light, second ed., Princeton University Press, Princeton, 2008.

[11] M. Bellingeri, A. Chiasera, I. Kriegel, F. Scotognella, Optical properties of periodic, quasi-periodic, and disordered one-dimensional photonic structures, Opt. Mater. 72 (2017) 403–421, https://doi.org/10.1016/j.optmat.2017.06.033.

[12] P. Lova, G. Manfredi, D. Comoretto, Advances in functional solution processed planar 1D photonic crystals, Adv. Optic. Mater. 6 (2018) 1800730, https://doi.org/10.1002/adom.201800730.

[13] M.D. Tocci, M. Scalora, M.J. Bloemer, J.P. Dowling, C.M. Bowden, Measurement of spontaneous-emission enhancement near the one-dimensional photonic band edge of semiconductor heterostructures, Phys. Rev. A. 53 (1996) 2799–2803, https://doi.org/10.1103/PhysRevA.53.2799.

[14] D. Dovzhenko, D. Dovzhenko, D. Dovzhenko, I. Martynov, P. Samokhvalov, E. Osipov, M. Lednev, A. Chistyakov, A. Karaulov, I. Nabiev, I. Nabiev, I. Nabiev, I. Nabiev, Enhancement of spontaneous emission of semiconductor quantum dots inside one-dimensional porous silicon photonic crystals, Opt. Express, OE. 28 (2020) 22705–22717, https://doi.org/10.1364/OE.401197.

[15] T. Komikado, S. Yoshida, S. Umegaki, Surface-emitting distributed-feedback dye laser of a polymeric multilayer fabricated by spin coating, Appl. Phys. Lett. 89 (2006), https://doi.org/10.1063/1.2336740, 061123.

[16] F. Scotognella, A. Monguzzi, F. Meinardi, R. Tubino, DFB laser action in a flexible fully plastic multilayer, Phys. Chem. Chem. Phys. 12 (2009) 337–340, https://doi.org/10.1039/B917630F.

[17] F. Scotognella, D.P. Puzzo, M. Zavelani-Rossi, J. Clark, M. Sebastian, G.A. Ozin, G. Lanzani, Two-photon poly(phenylenevinylene) DFB laser, Chem. Mater. 23 (2011) 805–809, https://doi.org/10.1021/cm102102w.

[18] V. Robbiano, G.M. Paternò, A.A. La Mattina, S.G. Motti, G. Lanzani, F. Scotognella, G. Barillaro, Room-Temperature low-threshold lasing from monolithically integrated nanostructured porous silicon hybrid microcavities, ACS Nano 12 (2018) 4536–4544, https://doi.org/10.1021/acsnano.8b00875.

[19] Y. Lu, Z. Lowther, N.D. Christianson, Z. Li, E. Baer, M.G. Kuzyk, N.J. Dawson, Demonstration of a self-healing all-polymer distributed Bragg reflector laser, Appl. Phys. Lett. 116 (2020) 103301, https://doi.org/10.1063/1.5145148.

[20] Z.V. Vardeny, A. Nahata, A. Agrawal, Optics of photonic quasicrystals, Nat. Photonics 7 (2013) 177–187, https://doi.org/10.1038/nphoton.2012.343.

[21] D.S. Wiersma, Disordered photonics, Nat. Photonics 7 (2013) 188–196, https://doi.org/10.1038/nphoton.2013.29.

[22] M. Bellingeri, F. Scotognella, Light transmission behaviour as a function of the homogeneity in one dimensional photonic crystals, Photon. Nanostruct. Fundamentals Appl. 10 (2012) 126–130, https://doi.org/10.1016/j.photonics.2011.08.006.

[23] V. Milner, A.Z. Genack, Photon localization laser: low-threshold lasing in a random amplifying layered medium via wave localization, Phys. Rev. Lett. 94 (2005), https://doi.org/10.1103/PhysRevLett.94.073901, 073901.

[24] W. Zhang, M. Anaya, G. Lozano, M.E. Calvo, M.B. Johnston, H. Míguez, H.J. Snaith, Highly efficient perovskite solar cells with tunable structural color, Nano Lett. 15 (2015) 1698–1702, https://doi.org/10.1021/nl504349z.

[25] P. Lova, P. Giusto, F. Di Stasio, G. Manfredi, G.M. Paternò, D. Cortecchia, C. Soci, D. Comoretto, All-polymer methylammonium lead iodide perovskite microcavities, Nanoscale 11 (2019) 8978–8983, https://doi.org/10.1039/C9NR01422E.

[26] A.M.A. Leguy, Y. Hu, M. Campoy-Quiles, M.I. Alonso, O.J. Weber, P. Azarhoosh, M. van Schilfgaarde, M.T. Weller, T. Bein, J. Nelson, P. Docampo, P.R.F. Barnes, Reversible hydration of CH3NH3PbI3 in films, single crystals, and solar cells, Chem. Mater. 27 (2015) 3397–3407, https://doi.org/10.1021/acs.chemmater.5b00660.

[27] P. Löper, M. Stuckelberger, B. Niesen, J. Werner, M. Filipič, S.-J. Moon, J.-H. Yum, M. Topič, S. De Wolf, C. Ballif, Complex refractive index spectra of CH3NH3PbI3 perovskite thin films determined by spectroscopic ellipsometry and spectrophotometry, J. Phys. Chem. Lett. 6 (2015) 66–71, https://doi.org/10.1021/jz502471h.

[28] L.J. Phillips, A.M. Rashed, R.E. Treharne, J. Kay, P. Yates, I.Z. Mitrovic, A. Weerakkody, S. Hall, K. Durose, Dispersion relation data for methylammonium lead triiodide perovskite deposited on a (100) silicon wafer using a two-step vapour-phase reaction process, Data in Brief 5 (2015) 926–928, https://doi.org/10.1016/j.dib.2015.10.026.

[29] L.J. Phillips, A.M. Rashed, R.E. Treharne, J. Kay, P. Yates, I.Z. Mitrovic, A. Weerakkody, S. Hall, K. Durose, Maximizing the optical performance of planar CH3NH3PbI3 hybrid perovskite heterojunction stacks, Sol. Energy Mater. Sol. Cell. 147 (2016) 327–333, https://doi.org/10.1016/j.solmat.2015.10.007.

[30] B. Song, J. Hou, H. Wang, S. Sidhik, J. Miao, H. Gu, H. Zhang, S. Liu, Z. Fakhraai, J. Even, J.-C. Blancon, A.D. Mohite, D. Jariwala, Determination of dielectric functions and exciton oscillator strength of two-dimensional hybrid perovskites, ACS Mater. Lett. 3 (2021) 148–159, https://doi.org/10.1021/acsmaterialslett.0c00505.

[31] M. Born, E. Wolf, A.B. Bhatia, P.C. Clemmow, D. Gabor, A.R. Stokes, A.M. Taylor, P.A. Wayman, W.L. Wilcock, Principles of Optics: Electromagnetic Theory of Propagation, Interference and Diffraction of Light, seventh ed., Cambridge University Press, 1999 https://doi.org/10.1017/CBO9781139644181.

[32] M. Bellingeri, I. Kriegel, F. Scotognella, One dimensional disordered photonic structures characterized by uniform distributions of clusters, Opt. Mater. 39 (2015) 235–238, https://doi.org/10.1016/j.optmat.2014.11.033.

[33] X. Xiao, W. Wenjun, L. Shuhong, Z. Wanquan, Z. Dong, D. Qianqian, G. Xuexi, Z. Bingyuan, Investigation of defect modes with Al2O3 and TiO2 in one-dimensional photonic crystals, Optik 127 (2016) 135–138, https://doi.org/10.1016/j.ijleo.2015.10.005.

[34] I.H. Malitson, Interspecimen comparison of the refractive index of fused silica*,†, J. Opt. Soc. Am., JOSA. 55 (1965) 1205–1209, https://doi.org/10.1364/JOSA.55.001205.
[35] F. Scotognella, A. Chiasera, L. Criante, E. Aluicio-Sarduy, S. Varas, S. Pelli, A. Łukowiak, G.C. Righini, R. Ramponi, M. Ferrari, Metal oxide one dimensional photonic crystals made by RF sputtering and spin coating, Ceram. Int. 41 (2015) 8655–8659, https://doi.org/10.1016/j.ceramint.2015.03.077.
[36] X. Jiang, Y. Zhang, S. Feng, K.C. Huang, Y. Yi, J.D. Joannopoulos, Photonic band gaps and localization in the Thue–Morse structures, Appl. Phys. Lett. 86 (2005) 201110, https://doi.org/10.1063/1.1928317.
[37] C. Toccafondi, L. Occhi, O. Cavalleri, A. Penco, R. Castagna, A. Bianco, C. Bertarelli, D. Comoretto, M. Canepa, Photochromic and photomechanical responses of an amorphous diarylethene-based polymer: a spectroscopic ellipsometry investigation of ultrathin films, J. Mater. Chem. C. 2 (2014) 4692–4698, https://doi.org/10.1039/C4TC00371C.